Observation of isotropic giant magnetoresistance in paramagnetic Au80 Fe20

PHYSICAL REVIEW B, VOLUME 63, 180404(R)

# Observation of isotropic giant magnetoresistance in paramagnetic $Au_{80}Fe_{20}$

Paolo Allia,[1] Marco Coisson,[2] Vincenzo Selvaggini,[1] Paola Tiberto,[3] and Franco Vinai[3]
[1]*Dipartimento di Fisica, Politecnico di Torino, and INFM, Research Unit Torino Politecnico, Corso Duca degli Abruzzi 24, I-10129 Torino, Italy*
[2]*DISPEA, Politecnico di Torino, and INFM, Corso Duca degli Abruzzi 24, I-10129 Torino, Italy*
[3]*Istituto Elettrotecnico Nazionale Galileo Ferraris and INFM, Research Unit Torino Politecnico, Corso Massimo d'Azeglio 42, I-10125 Torino, Italy*

(Received 2 February 2001; published 20 April 2001)

Magnetization and magnetoresistance were measured at room temperature and above on $Au_{80}Fe_{20}$ platelets and ribbons obtained by solid-state quenching and melt spinning. The as-quenched samples contain a solid solution of Fe in Au and exhibit a paramagnetic (Curie-Weiss) behavior in the considered temperature range; magnetic data indicate very short-ranged magnetic correlation among adjacent spins, enhanced by local composition fluctuations. The solid solution is very stable. Only a very limited fraction (never exceeding 1%) of nanometer-sized, bcc Fe particles appears after long-time isothermal anneals at suitable temperatures. A negative magnetoresistance was observed at room temperature in all examined samples. The observed effect is anhysteretic, isotropic, and quadratically dependent on magnetic field $H$ and magnetization $M$. The signal scales with $M$ rather than with $H$, indicating that it depends on the field-induced magnetic order of the Fe moments, as it does for conventional giant magnetoresistance in granular magnetic systems. This effect derives from spin-dependent scattering of conduction electrons from single Fe spins or very small Fe clusters. The scattering centers are almost uncorrelated at a distance of the order of the electronic mean free path (of the order of 1.5 nm, or a few atomic spacings, at RT).

DOI: 10.1103/PhysRevB.63.180404 PACS number(s): 75.50.Tt, 75.20.En, 75.75.+a

## I. INTRODUCTION

The $Au_{100-x}Fe_x$ magnetic system has been studied for many decades owing to its notable magnetic properties at low and high temperature, including magnetic cluster formation, spin-/cluster glass behavior, mictomagnetism, and superparamagnetism in various ranges of Fe concentration.[1–4] However, comparatively few studies on magnetotransport properties of AuFe/AuFeNi alloys are found in the literature,[5–8] and room-temperature data for bulk granular alloys are lacking. Room-temperature results have instead been reported for a few Fe/Au multilayered films.[9,10] Au-based bulk materials, such as AuCo and AuCoB heterogeneous alloys, exhibit at room temperature a magnetoresistance (MR) having the same origin as in other granular systems (Cu-Co, Ag-Fe, and Cu-Fe).[11] The MR of heterogeneous bulk systems containing nanometer-sized particles of a ferromagnetic metal is intimately connected with the process of magnetic ordering in these materials (often exhibiting high-temperature superparamagnetism) and may be exploited to get information about magnetic correlations extending over the scale of the electronic mean free path (mfp).[12] However, no definite tendency towards segregation of nanometer-sized particles of bcc Fe is exhibited by the AuFe system; this circumstance has possibly prevented systematic investigation of MR so far.

## II. EXPERIMENT

$Au_{80}Fe_{20}$ alloys were produced either by rapid solidification from the melt (using a standard melt-spinning apparatus in vacuum) or by solid-state quenching. In the first case, continuous ribbons were formed (width 2 mm; average thickness 120 $\mu$m), while platelets obtained by solid-state quenching were subsequently laminated to a thickness of 150 $\mu$m. The samples for magnetic and electrical measurements were produced either by cutting ribbon pieces or by platelet punching. The composition (routinely verified by scanning electron microscopy and lattice-constant measurements through x-ray diffraction) was chosen in order to deal with a paramagnetic system at room temperature and above [the Curie temperature of homogeneous $Au_{80}Fe_{20}$ occurs at 290 K (Ref. 13)]. Furnace anneals of as-prepared samples were performed in a controlled atmosphere. The prepared alloys were examined by TEM and small-angle neutron scattering (SANS) (PAPOL, Laboratoire Léon Brillouin, Saclay) in order to check for the presence of Fe precipitates.

Magnetic measurements were performed in the ranges $300\ \text{K} \leqslant T \leqslant 620\ \text{K}$ and $-20\ \text{kOe} \leqslant H \leqslant +20\ \text{kOe}$ through a vibrating-sample magnetometer (VSM), and in the ranges $5\ \text{K} \leqslant T \leqslant 300\ \text{K}$ and $-50\ \text{kOe} \leqslant H \leqslant +50\ \text{kOe}$ through an extraction method with a superconducting magnet. MR measurements were done by means of a standard four-probe technique with soldered contacts, using the VSM's electromagnet. The measuring temperature was monitored by a compensated thermocouple placed in close proximity to the sample (high-temperature measurements) and by a calibrated CERNOX sensor (low-temperature measurements).

## III. RESULTS

### A. Magnetic properties

X-ray-diffraction, SANS, and TEM data coherently indicate that both as-quenched ribbons and as-prepared platelets contain a homogeneous solid solution of Fe in Au, without

 

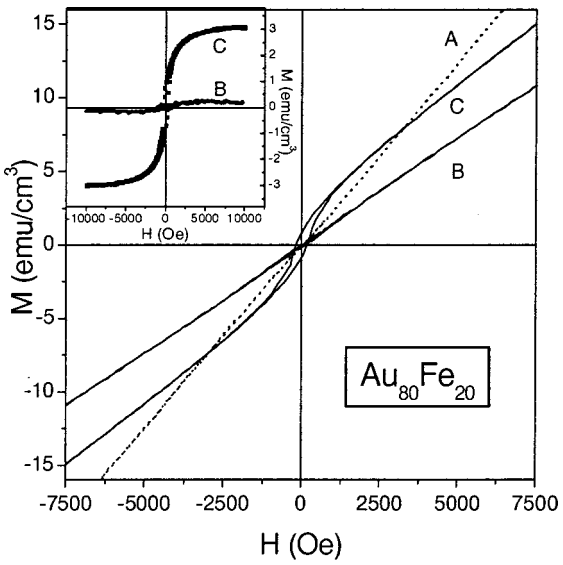


FIG. 1. Room-temperature magnetization curves of $Au_{80}Fe_{20}$ alloys around $H=0$; (*A*) as-quenched ribbon; (*B*) as-quenched platelet; (*C*) annealed ribbon (673 K, 16 h and 773 K, 16 h); (inset) hysteretic magnetization observed in (*B*) and (*C*) samples after subtracting the paramagnetic straight line.

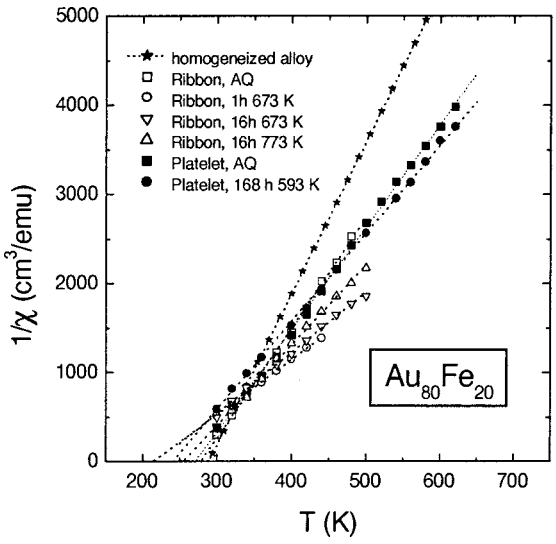


FIG. 2. Plots of $1/\chi$ vs $T$ for $Au_{80}Fe_{20}$ ribbons/platelets and for the homogeneous alloy (see legend).

any evidence of nanometer-sized Fe particles or smaller superparamagnetic (SP) clusters (as did the platelets or disks containing up to some hundreds of atoms, often found in similar alloys of the Au-Fe system[4,6]). The solid solution obtained through the adopted preparation techniques is rather stable against precipitation of large-scale Fe particles. Although a faint change in the lattice constant was observed by x-ray diffraction, indicating some segregation of Fe atoms, neither Fe particles nor Fe clusters were observed by TEM and SANS even after long-time anneals at temperatures well below the *solvus* temperature ($\leqslant 793$ K), specifically chosen in order to possibly enhance the tendency towards sample heterogenization [higher annealing temperatures ($T_a = 1170$ K) must be used to obtain fully homogeneous materials[13]]. However, local atomic rearrangements responsible for reversible and/or irreversible changes in the local magnetic properties have been observed even at room temperature in alloys of the AuFe system.[14,15]

Typical room-temperature magnetization curves for the as-quenched ribbon (*A*) and the as-quenched, laminated platelet (*B*) are shown in Fig. 1. The $M(H)$ dependence in the ribbon is linear over the entire magnetic-field range, with no detectable hysteresis, indicating a pure paramagnetic behavior. A small hysteresis superimposed on the paramagnetic straight line is observed in the as-quenched platelet ($B$), indicating a very small fraction of bcc Fe precipitates, undetected by TEM and SANS. A significant change in the slope of samples *A* and *B*, clearly related to the different preparation techniques, is observed. After low-temperature annealing of the platelet (16 h at 673 K and 16 h at 773 K), a more definite hysteretic behavior appears ($C$), again superimposed on the paramagnetic straight line and indicating precipitation of ferromagnetic bcc Fe particles. The hysteretic behavior is best viewed by subtracting the dominant paramagnetic contribution from the raw experimental data, as shown in Fig. 1 (bottom) for the as-quenched and annealed platelets. The saturation magnetization of these loops provides a figure of the amount of precipitated bcc Fe. If all Fe atoms were packed into large ferromagnetic precipitates, the alloy's saturation magnetization would be 340 emu/cm$^3$ using parameter values appropriate to bulk Fe. Our results indicated that a very tiny fraction of Fe atoms actually belongs to SP bcc particles (0.09% and 0.95% of total Fe in as-quenched and annealed platelets, respectively). The anhysteretic curves obtained by these loops are fitted by a single Langevin function, indicating a narrow distribution of SP moments. The resulting moments amount to $4550\mu_B$ for sample ($B$) and to $12\,800\mu_B$ for sample ($C$); the average interparticle distance is very large [52 nm for sample ($B$) and 33 nm for sample ($C$)]. As a matter of fact, x-ray data indicate that a slightly larger fraction of solute Fe atoms have precipitated after annealing as fcc antiferromagnetic Fe particles, which are not detectable by VSM. Even in this case, however, the maximum quantity of overall precipitated Fe never exceeds 1.6% of total solute Fe.[15] Assuming that the SP particle magnetization merely adds to the one from the solid solution, the magnetic properties of the latter are obtained by subtracting the hysteresis loops from the total $M(H)$ curves. The $1/\chi$ vs $T$ curves of a set of produced alloys (in the as-quenched and annealed conditions) are shown in Fig. 2 after such a subtraction. The curve for a homogeneous alloy of identical composition is reported for comparison.[13] A Curie-Weiss law is followed; the relevant magnetic properties are shown in Table I. Both the effective number of Bohr magnetons per magnetic unit $p_{eff}$ and the paramagnetic Curie temperature $T_C$ substantially differ from those of the homogeneous alloy. The values of $p_{eff}$ calculated using $N=1.21\times10^{22}$ atoms/cm$^3$ may be substantially higher than those found in the homogeneous system. On the other hand, $p_{eff}$ may be independently obtained by analyzing the alloy's saturation magnetization at low temperatures. The magnetization vs field curve measured at 5 K on the as-quenched ribbon

TABLE I. Effective number of Bohr magnetons per magnetic atom $p_{eff}$ and paramagnetic Curie temperature $T_C$ for $Au_{80}Fe_{20}$ ribbons/platelets submitted to various anneals, and comparison with the fully homogenized alloy.

| | $p_{eff}$ | $T_C$ (K) | $n$ |
|---|---|---|---|
| Homogeneous alloy | 4.83 | 290 | 3.45 |
| Platelet, AQ | 5.88 | 272 | 5.11 |
| Ribbon, AQ | 5.01 | 286 | 3.71 |
| Platelet, annealed 168 h at 593 K | 6.35 | 240 | 5.96 |
| Ribbon, annealed 1 h at 673 K | 8.11 | 213 | 9.73 |
| Ribbon, annealed 16 h at 673 K | 7.67 | 220 | 8.70 |
| Ribbon, annealed 16 h at 773 K | 6.88 | 244 | 7.00 |

fully saturates at 295 emu/cm$^3$ for $H>25$ kOe. Consequently, the effective number of Bohr magnetons per magnetic atom turns out to be $p_{eff}=2.6\mu_B$. This value is exactly the one referred to as the best Fe moment value in the AuFe system.[16] High values of the $p_{eff}$ extracted from high-temperature data are usually explained invoking the existence of magnetic correlations over very short distances, giving rise to clusters of strongly coupled adjacent Fe spins, coherently rotating under the influence of an external magnetic field, and constituting the true magnetic units of the system.[1,4] The weaker interaction existing among these units may be responsible for the reduced $T_C$ values. Assuming that all Fe spins in a cluster are ferromagnetically coupled, the average number $n$ of spins per cluster can be estimated using the following relation: $\mu_{CW}=n^{1/2}\mu_1$, where $\mu_1$ is the ''true'' moment ($2.6\mu_B$) while $\mu_{CW}$ is the value obtained from the Curie-Weiss analysis. The resulting $n$ values are reported in Table I. These data support the hypothesis that a substantial fraction of spins are magnetically coupled over very short distances. Larger values of $n$ would be obtained if the spins were not ferromagnetically aligned within clusters; the MR data indicate however that $n$ cannot be substantially larger than the present estimates (see below).

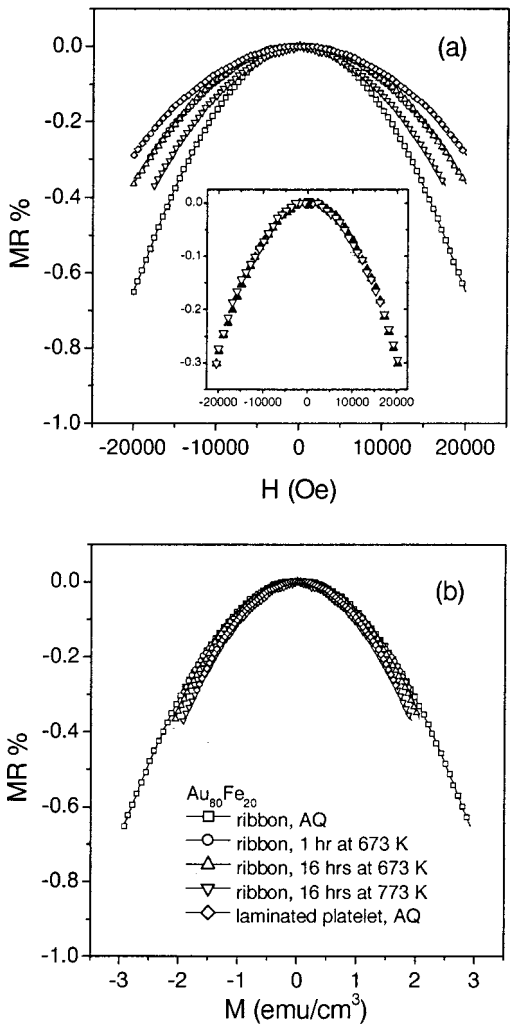


FIG. 3. Room-temperature magnetoresistance (MR) curves of $Au_{80}Fe_{20}$ (platelets/ribbons in the AQ condition and after thermal treatments; see legend); (a) MR vs $H$; (b) MR vs $M$. Inset in (a): results obtained on AQ $Au_{80}Fe_{20}$ platelet in perpendicular (full symbols) and transverse (open symbols) measuring conditions.

### B. Magnetoresistance

The $Au_{80}Fe_{20}$ alloy exhibits a room-temperature negative MR even in the absence of any detectable SP contribution to the magnetization curve. Typical room-temperature curves are shown in Fig. 3. The highest MR value is around 0.65% at 20 kOe. The main features of these MR curves are the following: the effect is isotropic [see the inset in Fig. 3(a), where the data taken on the as-quenched (AQ) platelet in the transverse and perpendicular configurations are superimposed] and anhysteretic, even in those samples where a small magnetic hysteresis is present; the MR follows a nearly perfect parabolic law when plotted against both $H$ and magnetization $M$; the MR scales with $M$ rather than with $H$: the curves almost (if not perfectly) overlap when plotted against $M$ [Fig. 3(b)]; and this means that the alloy's resistivity essentially depends on the field-induced magnetic order of the Fe moments. All these findings indicate that this effect is similar to the giant magnetoresistance (GMR) observed in granular bulk systems and granular thin films[4] containing large (nanometer-sized) SP particles. The origin of the MR in the present alloy is therefore the same as in heterogeneous granular systems, i.e., spin-dependent electronic scattering of conduction electrons from magnetic atoms; however, in the present case, the magnetic scatterers are not TM atoms at the interfaces between the matrix and nanometer-sized SP particles,[17,18] but very small Fe clusters or single, paramagnetic Fe atoms diluted in the Au matrix. The GMR in granular systems arises when the mean distance between adjacent scatterers is comparable to the electronic mfp $\lambda$. In $Au_{80}Fe_{20}$, the room-temperature $\lambda$ (calculated using the experimental resistivity value $\rho=63\ \mu\Omega$ cm and taking one electron per Au atom in the Drude formula) turns out to be 1.5 nm, or less than 4 atomic distances. This estimate again indicates an atomic origin of the MR. As previously remarked, the observed GMR does not strictly follow a universal curve when plotted against magnetization. The present data are not enough to interpret the tiny differences in MR-curve concavities [Fig. 3(b)] in terms of different structural

or electronic parameters, such as average size/distance of scatterers and electronic mfp. Such a study, requiring a wider set of analyzed data, is left for future work.

Finally, the parabolic shape of the MR vs $M$ curves suggests that the spins of magnetic scatterers are essentially independent at a distance of the order of $\lambda$ (different from the case of most granular SP systems, where flat-top parabolas may indicate magnetic correlation[19]). On the other hand, the magnetic measurements discussed previously (see Fig. 2 and Table I) suggest a significant correlation of adjacent spins, however not extending over distances on the order of $\lambda$ (such a circumstance would destroy the MR effect). These two results, taken together, indicate that in the $Au_{80}Fe_{20}$ alloy the magnetic correlation among spins is rather effective at distances comparable to a single atomic spacing, while it becomes vanishingly small over distances on the order of $\lambda$ (a few atomic distances), so that the system appears as more or less magnetically correlated, depending on the type of measurement performed. The effect of thermal fluctuations on MR in the paramagnetic phase of $Au_{80}Fe_{20}$ deserves further investigation. In fact, both the electronic mfp and the short-range magnetic order within clusters are expected to be reduced (possibly at different rates) on increasing $T$, affecting the MR value in a complex way. The experimental behavior of $1/\chi$ vs $T$ indicates that $p_{eff}$ is stable at least up to 640 K, so that in the initial temperature interval ($T_C \leqslant T \leqslant 640$ K) the changes in MR should be dominated by the electronic mfp.

## ACKNOWLEDGMENTS

The authors would like to thank M. Baricco (IFM Department, University of Torino) and A. Deriu (Physics Department, University of Parma) for providing the TEM and SANS data, respectively. This work was performed with the partial support of INFM-PRA ELTMAG.

[1] G. Zibold, in *Magnetic Properties of Metals*, Landolt-Börstein, New Series, Group III, Vol. 17, Pt. b, edited by H. J. Wijn (Springer-Verlag, Berlin, 1987), and references therein.
[2] A. P. Murani, J. Phys. F: Met. Phys. **4**, 757 (1974).
[3] P. A. Beck, Solid State Commun. **34**, 581 (1980).
[4] P. A. Beck, Phys. Rev. B **28**, 2516 (1983).
[5] J. Q. Wang, P. Xiong, and G. Xiao, Phys. Rev. B **47**, 8341 (1993).
[6] J. Xu *et al.*, Phys. Rev. B **56**, 14 602 (1997).
[7] Anindita Ray, R. Ranganathan, and C. Bansal, Phys. Rev. B **56**, 6073 (1997).
[8] Chen Xu and Zhen-Ya Li, J. Magn. Magn. Mater. **206**, 113 (1999).
[9] K. Shintaku, N. Hosoito, and T. Shinjo, J. Magn. Magn. Mater. **121**, 413 (1993).
[10] S. Honda, K. Koguma, M. Nawate, and I. Sakamoto, J. Appl. Phys. **82**, 4428 (1997).
[11] R. von Helmolt, J. Wecker, and K. Samwer, Appl. Phys. Lett. **64**, 791 (1994).
[12] P. Allia, M. Knobel, P. Tiberto, and F. Vinai, Phys. Rev. B **52**, 15 398 (1995).
[13] E. Scheil, H. Specht, and E. Wachtel, Z. Metallkd. **49**, 590 (1958).
[14] G. L. Whittle and S. J. Campbell, J. Phys. F: Met. Phys. **15**, 693 (1985).
[15] P. Allia *et al.*, in *Structure and Mechanical Properties of Nanophase Materials—Theory and Computer Simulations vs. Experiment*, edited by D. Farkas, H. Kung, M. Mayo, H. Van Swygenhoven, and J. Weertman, MRS Symposia Proceedings No. 634 (Materials Research Society, Warrendale, PA, 2001), p. B3.10.1.
[16] H. Okamoto, T. B. Massalski, L. J. Swartzendruber, and P. A. Beck, in *Phase Diagrams of Binary Fe Alloys*, edited by H. Okamoto (American Society for Metals, Materials Park, OH, 1993), p. 33.
[17] S. Zhang, Appl. Phys. Lett. **61**, 1855 (1992).
[18] T. A. Rabedeau *et al.*, Phys. Rev. B **48**, 16 810 (1993).
[19] P. Allia, P. Tiberto, and F. Vinai, Philos. Mag. B **76**, 447 (1997).